2,895,620 for 258 spectral points, whereas the hybrid method complexity is 64,512 for 1024 sampling points. The real test on a PC takes about five minutes to perform the third-order nonlinear simulation for the pure frequency-domain approach. The hybrid method only takes about six seconds to complete the same work.

5. CONCLUSION

In this paper, a hybrid method for Volterra analysis to simulate the weakly nonlinear characteristics of MESFET amplifiers for digital wireless communications systems has been proposed. The major modification is the time-domain equivalent baseband representation for the modulation signal, while the nonlinear calculations are still performed in the frequency-domain via Volterra expansions. Theoretical derivation indicates that complexity reduction can be achieved by using this hybrid approach. Numerical simulations showed the good agreement between the new and traditional approaches for the spectrum, ACPR, and EVM of the MESFET output signals with a large improvement in computation efficiency. The proposed method has potential applications for both circuit- and system-level simulations in digital wireless communications.

REFERENCES

1. J.J. Busogang, L. Ehrman, and J.M. Graham, Analysis of nonlinear systems with multiple inputs, Proc IEEE 62 (1974), 1088–1119.
2. M. Schetzen, The Volterra and Wiener theories of nonlinear systems, Wiley, New York, 1980.
3. C.L. Law and C.S. Aitchison, Prediction of wide-band power performance of MESFET distributed amplifiers using the Volterra series representation, IEEE Trans Microwave Theory Tech MTT-34 (1986), 1308–1317.
4. C.-C. Huang and T.-H. Chu, Analysis of MESFET injection-locked oscillators in fundamental mode of operation, IEEE Trans Microwave Theory Tech MTT-42 (1994), 1851–1857.
5. S.T. Chew and T. Itoh, Application of Volterra series to the problem of self-oscillating mixer, IEEE Microwave Theory Tech MTT-44 (1996), 269–274.
6. L. Hanzo, W. Webb, and T. Keller, Single- and multi-carrier quadrature amplitude modulation, principles and applications for personal communications, WLANs, and broadcasting, IEEE Press, New York, 2000.
7. J.F. Sevic and M.B. Steer, Analysis of GaAs MESFET spectrum regeneration driven by a π/4-DQPSK modulation source, IEEE Microwave Theory Tech Symp Dig, 1995, pp 1375–1379.
8. S.A. Maas, Volterra analysis of spectral regrowth, IEEE Microwave Guided Wave Lett 7 (1997), 192–193.
9. J.S. Kenney and A. Leke, Power amplifier spectral regrowth for digital cellular and PCS applications, Microwave J (1995), 74–92.
10. S.-W. Chen, W. Panton, and R. Gilmore, Effects of nonlinear distortion on CDMA communication systems, IEEE Microwave Theory Tech MTT-44 (1996), 2743–2750.
11. K.G. Gard, H.M. Gutierrez, and M.B. Steer, Characterization of spectral regrowth in microwave amplifiers based on the nonlinear transformation of a complex Gaussian process, IEEE Microwave Theory Tech MTT-47 (1999), 1059–1069.
12. C.-C. Huang, On the nonlinear distortion of QPSK-based digital modulation signals in microwave MESFET amplifiers, Microwave Opt Technol Lett 28 (2001), 212–214.
13. V.J. Mathews and G.L. Sicuranza, Polynomial signal processing, Wiley–Interscience, New York, 2000.
14. W.H. Press, B.P. Flannery, S.A. Tenkolsky, and W.T. Vetterling, Numerical recipes in C, Cambridge University Press, Cambridge, UK, 1988.
15. Telecommunications Industry Association, Cellular system dual-mode mobile-station base-station compatibility standard, EIA/TIA/IS-54-B Interim Standard, 1992.

BIAS-DEPENDENCE OF FET INTRINSIC NOISE SOURCES, DETERMINED WITH A QUASI-2D MODEL

A. Lázaro, M. C. Maya, and L. Pradell
Universitat Politècnica de Catalunya (UPC)
Dept. TSC, Campus Nord UPC
Mòdul D3, 08034, Barcelona, Spain

Received 30 April 2003

ABSTRACT: *The bias-dependence of microwave-FET intrinsic noise sources in their hybrid configuration is theoretically determined, using a new quasi-2D (Q-2D) physical model based on Thornber's current equation [8]. It is shown that the correlation coefficient cannot be neglected, in agreement with empirical work in the literature. Experimental verification using noise-parameter measurements up to 26 GHz is presented.* © 2003 Wiley Periodicals, Inc. Microwave Opt Technol Lett 39: 317–319, 2003; Published online in Wiley InterScience (www.interscience.wiley.com).

Key words: *FET noise models; FET quasi-2D models; FET intrinsic noise sources; noise parameters*

1. INTRODUCTION

The modelling of FET devices for CAD applications requires the determination of FET intrinsic noise sources and their frequency- and bias-dependence. Pospieszalski [1] proposed a two-parameter noise model in which the FET noise is described by two equivalent gate- and drain-noise temperatures, associated to uncorrelated gate-voltage and drain-current noise sources, respectively. This simple model predicts the frequency behaviour of device noise parameters with good accuracy. However, further work [2–4] has shown that inclusion of correlation in the voltage and current noise sources (hybrid model) may improve the agreement with experimental noise-parameter measurement results.

To theoretically investigate the behaviour of noise sources in their hybrid configuration, physical quasi-2D (Q-2D) simulators, such as those proposed in [5, 6], provide a cost-effective solution. While a Q-2D analysis has already been applied in [7] to the study of Pospieszalski's model, no theoretical studies on the bias dependence of the hybrid-model noise sources (including correlation), are available in the literature, to the authors' knowledge.

The purpose of this paper is to theoretically obtain the correlated hybrid noise sources and their bias dependence in arbitrary MESFET and HEMT devices, by using a new Q-2D model. In contrast to previous works, the Q-2D simulator presented here is based upon Thornber's current equation. This equation was suggested in [8] to include nonstationary effects (overshoot effect) due to the electric-field space gradient in short-gate devices (submicrometer FETs), but had not been applied to Q-2D models. This approach is a simpler, yet more accurate, alternative to the simultaneous solution of momentum and energy-conserving nonlinear equations proposed in [5, 6]. Local equivalent noise sources in the active channel are introduced in order to derive the device's intrinsic noise sources by using a nodal matrix method. Experimental verification up to 26 GHz is presented.

2. PHYSICAL, Q-2D BASED FET NOISE MODEL

The proposed Q-2D model for HEMTs is performed in two steps. The first step consists of charge-control and electron transport analysis to compute the DC-characteristics. The second step is the DC-model extension to analyse the device's noise parameters. Charge-control analysis is performed by solving Poisson's and

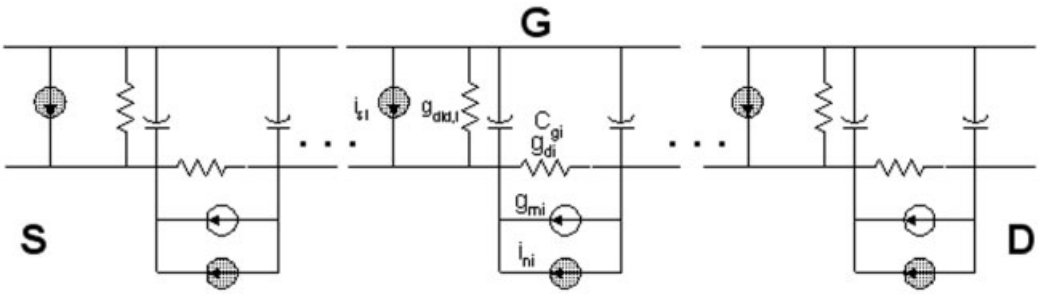

Figure 1 Distributed local equivalent-circuit of FET channel used to calculate *S* and noise parameters

Schrödinger's equations, simultaneously. Poisson's equation is solved numerically by using the Newton method to improve the convergence [6]. Therefore, any type of donor distribution in MESFETs, and arbitrary HEMTs (including multiple quantum-well structures), can be analysed. A lookup table for the channel-electron density is created for every gate-channel potential, and for any derivative of the longitudinal electric field dE_x/dx to compensate the large variations of E_x in the pinchoff region [6].

The electron transport analysis is accomplished by using Thornber's 1D generalised current equation. According to [8], the electron velocity can be expressed as the sum of a stationary electron velocity $v_s(E_x)$, a space-gradient term for modelling overshoot effects, and a diffusion term. For each channel layer k the electron velocity is given by

$$v_k(E_x) = v_{sk}(E_x) + W_k(E_x)\frac{\delta E_x}{\delta x} + D_k(E_x)\frac{1}{n_{sk}(x)}\frac{\delta n_{sk}(x)}{\delta x}, \quad (1)$$

where $n_s(x)$ is the channel electron density, $W(E_x)$ is the gradient coefficient, and $D(E_x)$ is the diffusion coefficient. For every longitudinal section i, the channel current is then expressed as

$$I_{ch,i} \approx qZ\sum_k n_{sk,i}v_{sk}(E_{x,i}) + qZ\sum_k n_{sk,i}W_k(E_{x,i-1})\frac{E_{x,i}-E_{x,i-1}}{\Delta x} + qZ\sum_k D(E_{x,i-1})\frac{n_{sk,i}-n_{sk,i-1}}{\Delta x}, \quad (2)$$

where Z is the channel width, q is the electron charge, and Δx is the section length. The procedure to obtain the DC drain characteristics is as follows. Given a drain current and a gate voltage, the electron density $n_{sk,i}$ for the actual section i (starting from the source side of the channel) is determined from the lookup table, and the electric field E_{xi} is solved using Eq. (2). Then, the channel voltage and the electron density for the next section $i + 1$ are updated. The procedure is repeated until the drain side of the channel and the drain voltage are computed.

The last step in an extension of the obtained DC-model to analyse noise parameters, by using the distributed local equivalent-circuit approach [5] see Fig. 1). Two main local noise sources at microwave frequencies are considered at every channel section, diffusion noise i_{ni} and shot noise i_{si}. Their spectral densities are known, respectively, from the local diffusion coefficient and electron density, and from the local gate current. Intrinsic Y parameters and admittance noise correlation matrix C_Y are obtained from the local equivalent circuit, using a nodal method. Finally, the hybrid noise-matrix C_H is computed from C_Y using well-known matrix transformations, and parasitic effects are included to obtain the device extrinsic S and noise parameters.

3. MODEL APPLICATION AND EXPERIMENTAL VALIDATION

The proposed Q-2D model has been applied to the simulation of a double-pulse-doped (DPD) HEMT with 0.3-μm gate length. Figure 2 compares its simulated noise parameters as a function of frequency (obtained using the Q-2D model proposed) with its measured noise parameters obtained with authors' tuner-based [9] and source-matched F_{50} [4, 10] methods. The excellent agreement between simulations and experimental results illustrates the model validity, accuracy, and usefulness applied to any type of submicrometer HEMTs. In Figure 3, the intrinsic hybrid noise matrix as a function of drain current is simulated for a 0.5-μm gate length conventional HEMT structure, but the conclusions may be extrapolated to any FET structure. The bias behaviour of matrix elements is exactly that predicted in previously reported experimental results [4], namely: (i) a linear dependence of drain spectral density (C_{H22}) with drain current is observed; (ii) the real part of the correlation coefficient $Re(\rho_H)$ at high drain currents is important [7]; (iii) the imaginary part of the correlation coefficient $Im(\rho_H)$ is nearly zero and can be neglected.

4. CONCLUSION

An accurate and flexible Q-2D model for submicrometer FETs has been presented. The simulator is based on Thornber's current equation to include nonequilibrium electron transport. The simulator has successfully been applied to obtain FET noise parameters and the bias behaviour of its hybrid noise model. Simulation

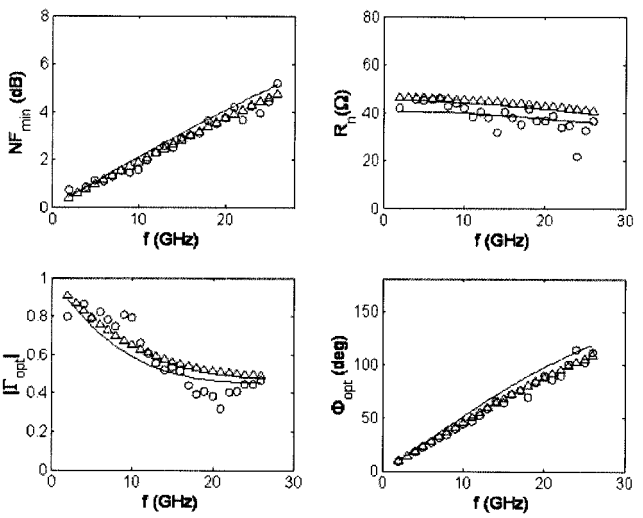

Figure 2 Comparison between simulated and measured noise parameters of a 0.3-μm gate-length DPD HEMT. Simulation (−); measurement using a tuner-based method [9] (o), measurement using the F_{50} technique [4, 10] (Δ)

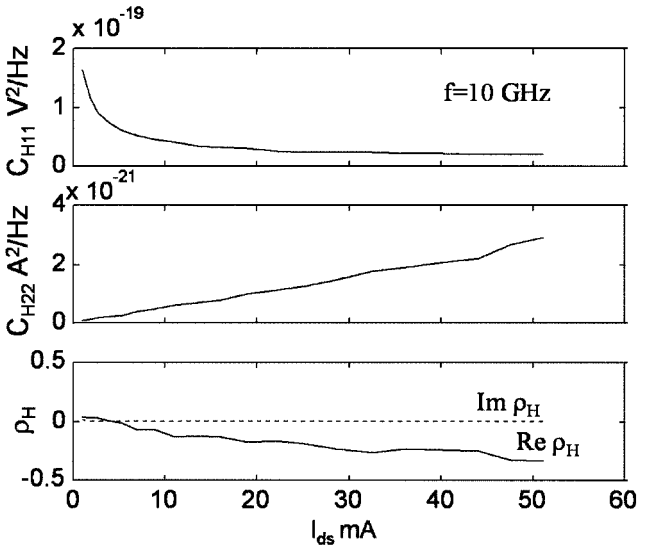

Figure 3 Drain-current dependence of hybrid correlation matrix C_H of a 0.5-μm gate-length conventional HEMT

results demonstrate that the real part of correlation coefficient at high-drain current is important. Experimental results up to 26 GHz using two different measurement methods confirm the simulations.

ACKNOWLEDGMENT

This work has been supported by Spanish Government under grants nos. TIC2000-0144-P4-02 and ESP2002-04141-C03-02 (MYCT), and a scholarship from CONACYT, Mexico.

REFERENCES

1. M.W. Pospieszalski, Modeling of noise parameters of MESFETs and MODFETs and their frequency and temperature dependence, IEEE Trans Microwave Theory Tech 37 9 (1989), 1340–1350.
2. R.A. Pucel, W. Struble, R. Hallgren, and U.L. Rohde, A general noise de-embedding procedure for packaged two-port linear active devices, IEEE Trans Microwave Theory Tech 40 (1992), 2013–2023.
3. H. Jong-Hee and K. Lee, A new extraction method for noise sources and correlation coefficient in MESFET, IEEE Trans Microwave Theory Tech 44 (1996), 487–492.
4. A. Lázaro, L. Pradell, and J.M. O'Callaghan, FET noise parameter determination using a novel technique based on 50Ω noise figure measurements, IEEE Trans Microwave Theory Tech 47 (1999), 315–324.
5. H. Happy, O. Pribetich, G. Dambrine, J. Alamkan, J. Cordier, and A. Cappy, HELENA: A new software for the design of MMICS, IEEE MTT-S Int Microwave Symp Dig 1991, pp. 627–630.
6. R. Singh, and C.M. Snowden, Small-signal characterisation of microwave and millimeter-wave HEMT's based on a physical model, IEEE Trans Microwave Theory Tech 44 (1996), 114–121.
7. F. Danneville, H. Happy, G. Dambrine, J. Belquin, and A. Cappy, Microscopic noise modelling and macroscopic noise models: How good a connection?, IEEE Trans Electron Dev 41 (1994), 779–785.
8. K.K. Thornber, Current equations for velocity overshoot, IEEE Electron Dev Lett 3 (1982), 69–71.
9. A. Lázaro, L. Pradell, and J.M. O'Callaghan, Novel method from measuring noise parameters of microwave two-port, IEE Electronics Lett 34 (1998), 1332–1333.
10. A. Lázaro, and L. Pradell, Extraction of the noise parameters of a transistor by using a spectrum analyser and 50Ω noise figure measurements only, IEE Electronic Lett 34 (1998), 2353–2354.

L-BAND ACTIVE RECEIVING ANTENNA FOR AUTOMOTIVE APPLICATIONS

Victor Rabinovich
Tenatronics Ltd.
Newmarket, Ontario,
Canada

Received 25 April 2003

ABSTRACT: *This paper describes L-band active receiving antenna for the automotive applications (DAB radio). The antenna is based on a printed dipole in 1452-1492 MHz frequency range and has a low noise amplifier. Two different versions of the antenna are presented: one for "on-vehicle" application (roof or trunk) and the second one for "in-vehicle" application (glass window). Antenna directionality is measured for on-vehicle and in-vehicle antenna locations.* © 2003 Wiley Periodicals, Inc. Microwave Opt Technol Lett 39: 319–323, 2003; Published online in Wiley InterScience (www.interscience.wiley.com). DOI 10.1002/mop.11203

Key words: *active antenna; low-noise amplifier; printed dipole; DAB radio*

1. INTRODUCTION

Microwave antennas integrated with the active elements—or active antennas—have received wide interest in mobile communications [1–4]. These antennas have the advantages of low cost, low profile, and light weight. This paper concerns two different versions of an active antenna for digital audio broadcasting radio (DAB) in the L-band frequency range. One of these active antennas can be used for "on-vehicle applications" and another one can be used for "in-vehicle" applications.

It is known that antenna pattern performances are very specific to the vehicle antenna location [5–7]. Reflections and shadowing effects can significantly change the antenna pattern. In contrast to the simulated results of the antenna on an ideal circular ground plane, only measurements of the antenna on the exact mounting location on the vehicle can show the real antenna performance. Therefore, a variety of measurements performed to study those effects in the DAB frequency band are presented in this paper.

2. ACTIVE ANTENNA SYSTEM DESIGN

As an antenna element, a printed on a thin dielectric substrate monopole is used. A surface-mounted low-profile omnidirectional monopoles are one of the popular types of antennas with vertical polarization performance [8–12]. The proposed antennas are fabricated on a cheap RF material FR-4 substrate with $\varepsilon_r = 4.5$. The substrate thickness is 1.6 mm. Figures 1 and 2 show two different antenna proposals. The first quarter wavelength antenna shown in Figure 1 is preferable for "on-vehicle" applications. Such an antenna can be used as the roof or trunk antenna. The second proposal, the bow-tie-shaped antenna shown in Figure 2 is preferable for "in-vehicle" applications. This antenna can be attached to the glass window. Extended ground in Figure 2 is used for 50Ω impedance matching. For the antenna shown in Figure 1, the amplifier circuit is arranged on the bottom side of the ground plane. According to Figure 2, the antenna patch and amplifier are placed on one side of a substrate, while the ground plane with extended ground parts is arranged on the other side of the substrate. The second antenna was designed and optimized for the L-band frequency range by using FEKO electromagnetic simulator [13]. Figures 3 and 4 show the measured input impedance and VSWR for these antennas without amplifiers.